Electronic characteristics of fluorene/TiO_2 molecular heterojunctions

Jing Wu[a)]
Department of Chemistry, The Ohio State University, Columbus, Ohio 43210

Ken Mobley
ZettaCore, Inc., Englewood, Colorado 80112

Richard L. McCreery[a),b)]
Department of Chemistry, The Ohio State University, Columbus, Ohio 43210

(Received 29 September 2006; accepted 21 November 2006; published online 10 January 2007)

The electronic properties of molecular junctions of the general type carbon/molecule/TiO_2/Au were examined as examples of "molecular heterojunctions" consisting of a molecular monolayer and a semiconducting oxide. Junctions containing fluorene bonded to pyrolyzed photoresist film (PPF) were compared to those containing Al_2O_3 instead of fluorene, and those with only the TiO_2 layer. The responses to voltage sweep and pulse stimulation were strongly dependent on junction composition and temperature. A transient current response lasting a few milliseconds results from injection and trapping of electrons in the TiO_2 layer, and occurred in all three junction types studied. Conduction in PPF/TiO_2/Au junctions is consistent with space charge limited conduction at low voltage, then a sharp increase in current once the space charge fills all the traps. With fluorene present, there is a slower, persistent change in junction conductance which may be removed by a reverse polarity pulse. This "memory" effect is attributed to a redox process in the TiO_2 which generates Ti^{III} and/or Ti^{II}, which have much higher conductance than TiO_2 due to the presence of conduction band electrons. The redox process amounts to "dynamic doping" of the TiO_2 layer by the imposed electric field. The memory effect arises from a combination of the properties of the molecular and oxide layers, and is a special property of the molecular heterojunction configuration. © *2007 American Institute of Physics*. [DOI: 10.1063/1.2423011]

INTRODUCTION

Electron transport (ET) through molecules in molecular junctions is fundamental to the area of molecular electronics, and understanding the relationship between molecular structure and transport is a prerequisite to the eventual design of molecular circuit components.[1,2] The factors which determine ET through molecules oriented between metallic contacts has been investigated in single molecule devices based on scanning probe microscopy,[3,4] as well as molecular junctions containing 10^3-10^{12} molecules in parallel.[5] It is clear from the results reported to date that ET depends on molecular structure as well as the nature of the "contacts" between the molecules and the conductors.[6,7] Several reviews on molecular junctions and molecular rectification have appeared, and research on ET mechanisms in such devices remains active.[2,4,8,9]

Several laboratories have investigated "hybrid" devices involving the interface between a molecule and a conventional semiconductor such as silicon, gallium arsenide, or TiO_2.[10] Research areas as diverse as dye sensitized solar cells and molecularly modified quantum dots also involve a combination of molecular and semiconductor properties.[11,12] Our laboratory has investigated carbon/molecular/TiO_2/Au junctions in some detail, and compared them to similar junctions lacking the TiO_2 layer.[6,8,13–18] By combining a molecular and semiconductor layer in the junction, one can in principle exploit the distinct electronic properties of each material in a "molecular heterojunction." For example, robust negative differential resistance has been observed in polyphenylene vinylene/TiO_2 heterojunctions,[19] with the phenomenon being attributed to alignment of energy levels between the polyphenylene vinylene and TiO_2. We have described carbon/nitroazobenzene (NAB)/TiO_2/Au junctions in which electrons are transferred between the NAB and TiO_2 to produce rectification and conductance switching.[8,13,14,16]

During both the spectroscopic and electronic characterizations of carbon/NAB/TiO_2/Au junctions, both transient and persistent conductance changes were observed, whose origin was not completely clear.[13,18] Potential pulses applied to such junctions produced a transient current lasting a few milliseconds, followed in some cases by a slow (10–100 ms) conductance increase which persisted for several minutes. This "memory" effect may have technological value as well as mechanistic consequences, and deserved further study. Although Raman spectroscopy established that NAB is reversibly reduced and oxidized in NAB/TiO_2 junctions only ~8 nm thick,[14,16] the fate of the TiO_2 accompanying NAB redox events was not amenable to Raman monitoring, and was not determined directly. It is clear from these investigations that electron injection into the TiO_2 film is directly

[a)]Present address: Department of Chemistry, University of Alberta, Alberta T6G, 2G2, Canada.
[b)]Author to whom correspondence should be addressed. Electronic mail: richard.mccreery@ualberta.ca

involved in the electronic behavior of the junction, but the events accompanying injection are not yet evident, including their relationship to observed changes in junction conductance.

The current investigation was undertaken to more clearly define the conductance changes which occur when carbon/molecule/TiO_2/Au heterojunctions are subjected to an applied electric field. Fluorene (FL) junctions were investigated rather than the previously studied NAB devices[14,16] in order to simplify the problem by reducing the possibility of redox reactions in the molecular layer. Carbon/FL/TiO_2/Au junctions were compared to carbon/TiO_2/Au analogs to determine the influence of the FL layer on electronic behavior. In addition, a carbon/Al_2O_3/TiO_2/Au junction was investigated as an analog with a high-barrier insulator in place of the FL layer.

EXPERIMENTAL

All junctions were of the "crossed junction" type which has been described in detail previously.[13,14,20] In all cases the junctions were formed at the intersection of a 1 mm wide strip of pyrolyzed photoresist film (PPF) and a 0.5 mm strip of Au and TiO_2 oriented perpendicular to the PPF to yield a junction area of 0.005 cm^2. PPF is structurally similar to glassy carbon, with <0.5 nm surface roughness and a resistivity of 0.006 Ω cm.[21] The TiO_2 was deposited from rutile with an electron beam evaporator at a rate of 0.03 nm/s. After initial pump down to $\sim 4\times10^{-6}$ torr, the e-beam chamber was backfilled with ultrahigh purity O_2 to $\sim 1\times10^{-5}$ torr during TiO_2 deposition. A residual gas analyzer (Stanford Research Systems RGA/200) determined the water and O_2 partial pressures to be typically 2.8×10^{-6} and 8×10^{-6} torr, respectively, before TiO_2 deposition, increasing to 1.3×10^{-5} and 2.0×10^{-5} torr during deposition. The thickness of the TiO_2 layer was determined by an atomic force microscopy (AFM) line profile of the pattern formed by TiO_2 deposition through a fine wire mesh to be 5.2 ± 0.25 nm. Au was deposited through the same shadow mask as the TiO_2 at 0.1 nm/s and a backpressure of 4×10^{-6} torr for a thickness of $\sim$12 nm, determined with a quartz crystal microbalance. X-ray photoelectron spectroscopy of the TiO_2 showed only Ti^{IV}, with no observable Ti^{II} or Ti^{III}. The fluorene layer was deposited on PPF from its diazonium ion precursor using conditions which yielded a monolayer with a thickness of 1.7 nm, as determined by AFM "scratching."[20,22] Junctions will be designated according to their composition as follows: PPF/FL/TiO_2/Au or PPF/Al_2O_3/TiO_2/Au. In all cases the thicknesses of various layers were as follows: PPF, 1–2 μm; FL, 1.7 nm; TiO_2, 5.2 nm; Al_2O_3, 3 nm; and Au, 12 nm.

Electronic characterization was performed with the "four-wire" configuration shown in Fig. 1. The actual bias across the junction was measured differentially by a LABVIEW data acquisition board, in order to correct for Ohmic voltage losses in the PPF and Au leads. The operational amplifier was useful for active compensation of PPF resistance, which was important for obtaining accurate voltage pulses. The current amplifier was a Stanford Research Systems

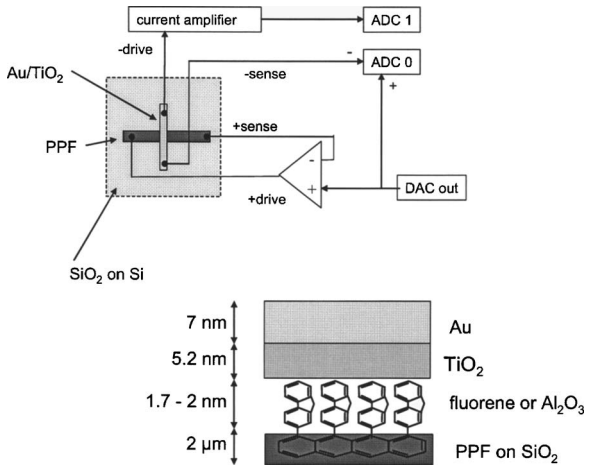

FIG. 1. Schematics of junction structure and instrumentation. Upper drawing is "four-wire" arrangement which corrects for Ohmic errors in leads of the "crossed junction" geometry. DAC applies the bias and ADC0 monitors the iR-corrected voltage across the junction. Lower drawing is the junction structure, with layer thicknesses. In several cases noted in the text, the fluorene layer was absent or replaced with Al_2O_3.

model 570, with a bandwidth of 1 MHz. For the experiments involving low temperature the sample was positioned on a LN_2 cooled copper stage heated by a cartridge heater controlled by a thermocouple positioned next to the sample. The J/V curves obtained as a function of temperature were acquired with a "three-wire" configuration, with the "sense" input the ADC0 being grounded, due to differences in the apparatus. In all figures, the voltage is plotted as PPF relative to Au, and the current as A/cm^2 for the 0.005 cm^2 junction area. Each sample had 8–12 junctions and approximately 1 out of 20 junctions was rejected due to anomalously high current density. For eight different PPF/FL/TiO_2/Au samples, the reproducibility of the accepted junctions was evaluated by determining the mean voltage at which the current density crossed 0.016 A/cm^2, along with the standard deviation of this voltage. For positive bias, the mean voltage was 2.19 ± 0.16 V, and for negative bias, it was 1.76 ± 0.20 V. All electronic characterization was carried out in ambient air. Junction resistance increased slowly following e-beam deposition, but stabilized in $\sim$1 week in ambient air, so junctions used for electronic characterization were between 1 and 4 weeks old. Completed junctions were sensitive to high humidity, but were stable when stored in a desiccator.

RESULTS

In all cases, the junctions investigated with current/voltage scans and pulse experiments were of three types which were prepared identically except for the "molecular" layer: PPF/TiO_2/Au, PPF/FL/TiO_2/Au, and PPF/Al_2O_3/TiO_2/Au. These cases were chosen to represent (1) a semiconducting oxide (TiO_2) alone, (2) a fluorene monolayer added to the TiO_2 layer, and (3) a high barrier oxide (Al_2O_3) substituted for the fluorene monolayer. Figures 2(A) and 2(B) show the J/V response as a function of scan rate for PPF/FL/TiO_2/Au molecular junctions. At high scan rate, the current density is relatively small over the

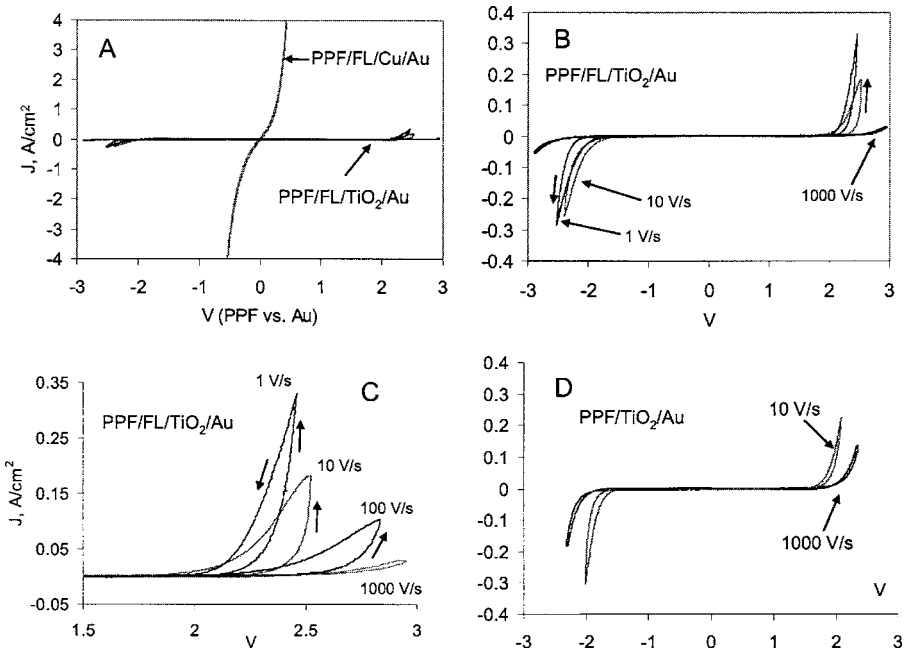

FIG. 2. Current density/voltage (J/V) curves for fluorene junctions at various scan rates. (A) FL/Cu (100 V/s) and FL/TiO_2 at 1, 10, and 1000 V/s, as indicated. All scans were initiated in positive direction from zero bias, and the voltage is PPF relative to Au. (B) Same as (A), but with expanded current density scale, and lacking FL/Cu curve. Arrows indicate scan direction. (C) PPF/FL/TiO_2/Au at four scan rates, but on expanded voltage scale. (D) PPF/TiO_2/Au at two scan rates.

range of ±3 V. Beyond 3 V at either polarity the junction broke down, even at 10^4 V/s, to yield a sudden, irreversible increase in current. A J/V response for a PPF/FL/Cu/Au junction containing 30 nm of Cu but no TiO_2 is included in Fig. 2(A) to show that the TiO_2 greatly attenuates the observed current.[20] At slower scan rates the current increased significantly for $|V|>2$ V, and showed substantial hysteresis [apparent in the expanded scales in Figs. 2(B) and 2(C)]. When the fluorene layer was absent [Fig. 3(D)] the scan rate dependence and the hysteresis were substantially less pronounced. As reported previously,[14] the fluorene junctions show minimal rectification, much weaker than that observed with a reducible molecule substituted for fluorene.[13,14]

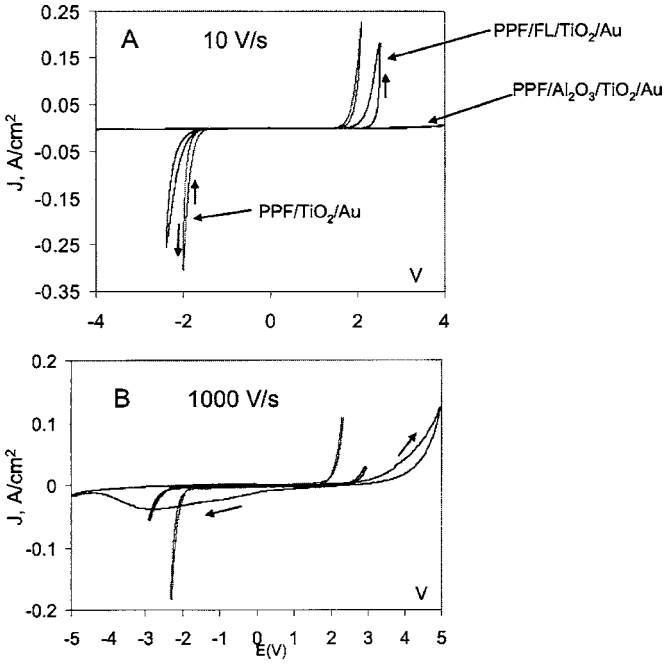

FIG. 3. J/V curves at two scan rates comparing PPF/FL/TiO_2/Au, PPF/Al_2O_3/TiO_2/Au, and PPF/TiO_2/Au junctions. Arrows indicate scan direction.

Current density/voltage (J/V) curves obtained at a relatively slow scan rate of 10 V/s are shown in Fig. 3(A) for the three junction types. The Al_2O_3/TiO_2 junction behaved as an insulator with a maximum current density <0.005 A/cm^2 over the range ±4 V. The TiO_2 junction had low conductance for the range of $-1.5<V<1.5$ with a sharp increase in current for $|V|>2$ V. The FL/TiO_2 junction exhibits similar behavior, but with a higher $|V|$ required for significant current density, and both the TiO_2 and FL/TiO_2 junctions exhibit hysteresis. For fast scans at 1000 V/s, the results for FL/TiO_2 and TiO_2 junctions were qualitatively similar to the 10 V/s scans, but with less hysteresis and a higher voltage where significant current densities were observed. The Al_2O_3/TiO_2 junction showed very different J/V behaviors at 1000 V/s than at 10 V/s, with a peak observed during the negative scan at approximately −3 V. The variation of J/V response with scan rate indicates a dynamic system, with the conductance changing during voltage scans to yield hysteresis. For example, during the positive scan at 10 V/s for the FL/TiO_2 case shown in Fig. 3(A), the current increases at ~2.4 V, then is larger during the negative going scan after reversal at +2.5 V than it was on the initial positive scan. This behavior is quite different from that observed for the analogous PPF/FL/Cu junction, in which the current is much larger (~5 A/cm^2 at 0.5 V), exhibits minimal hysteresis, and is invariant with scan rate or direction except for a capacitive component at high scan rates.[20]

Additional evidence for structural dynamics is provided by the temperature dependence shown in Fig. 4. FL/TiO_2 and TiO_2 junctions showed qualitatively similar changes with temperature, shown in Fig. 4(A) for the case of PPF/TiO_2/Au. For both junction types, the current decreases significantly at low temperature. At −135 °C the J/V curves are essentially identical for 10 and 1000 V/s [Fig. 4(B)], with the only difference being a small capacitive current component at high scan rate. The capacitance calculated from the current at $V=0$ and the scan rate decreased at lower

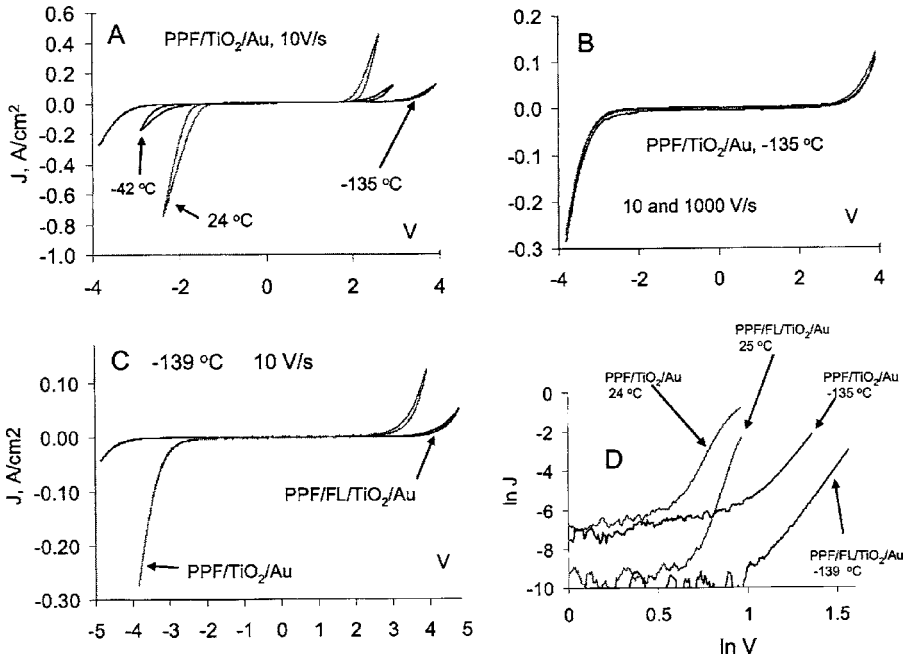

FIG. 4. Temperature dependence of J/V curves for molecular heterojunctions at two scan rates. (A) $PPF/TiO_2/Au$, 10 V/s at the temperatures indicated; (B) $PPF/TiO_2/Au$ at −135 °C, 10 and 1000 V/s; (C) $PPF/TiO_2/Au$ and $PPF/FL/TiO_2/Au$ junctions, both at −139 °C and 10 V/s; and (D) plots of $\ln J$ vs $\ln V$ for the initial positive scan of panel C. $\ln J$ values below −6 at 25 °C and −9 at −135 °C are not meaningful, due to dynamic range constraints of the current amplifier.

temperature and higher scan rate, indicating a pronounced frequency dependence. Note that relatively large current densities are observed (>0.2 A/cm^2) even at −135 °C, albeit at higher bias than required at 25 °C. In addition, hysteresis is nearly absent at −135 °C, but increases at higher temperatures. Figure 4(C) shows an overlay of TiO_2 and FL/TiO_2 junctions at low temperature, where the response is scan rate independent and the junctions appear to be structurally static. The fact that the J/V curves vary significantly with scan rate at room temperature but are independent of scan rate at −135 °C implies that whatever structural changes are responsible for the scan rate variation are "frozen out" at the lower temperatures. Figure 4(D) is a plot of $\ln(J)$ vs $\ln(V)$ for both junctions at room temperature and low temperature, as indicated. As noted in the Discussion section, the slopes of such plots provide clues about the conduction mechanism.

The pronounced scan rate dependence of FL/TiO_2 junctions apparent in Figs. 2(B) and 2(C) implies that the application of a voltage step to a fixed potential of 2–3 V should result in a current response which increases with time. Figure 5(A) shows the response to 100 ms pulses to ±2–3 V then back to $V=0$. After an initial current spike lasting of ~0.3 ms, the current density increases with time for $|V|>2$ V. We reported previously the relatively slow increase in current for nitroazobenzene/TiO_2 junctions, and attributed them to redox reactions within the junction.[13,16,18,23] As shown in Fig. 5(B) with faster time resolution, the initial current spike scales approximately with applied voltage. Although the slow response depends strongly on the composition of the junction [Fig. 5(C)], the fast transient does not vary greatly when FL or Al_2O_3 are present adjacent to the TiO_2 layer.

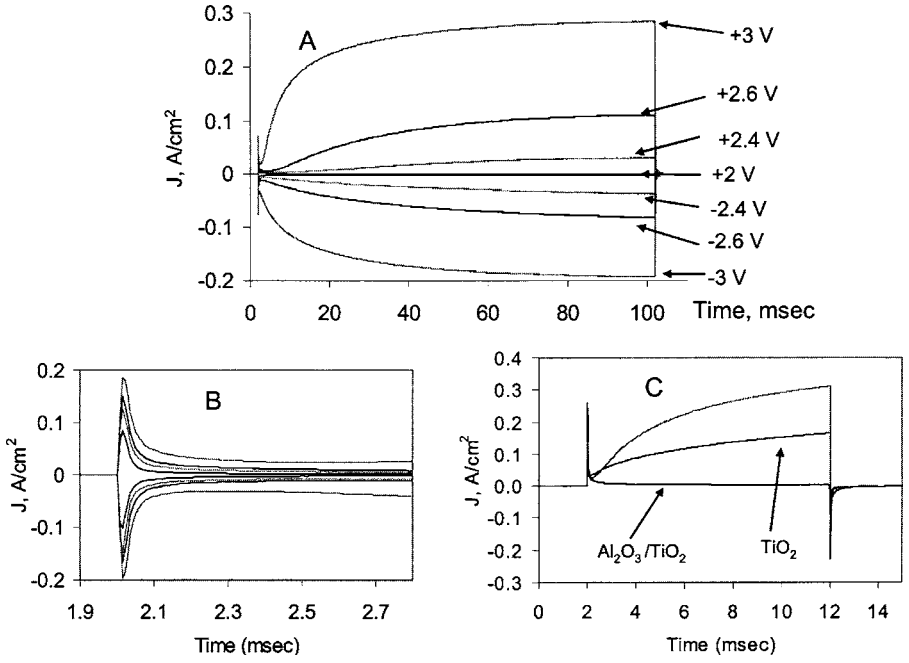

FIG. 5. Voltage pulses with 2–3 V amplitude applied to various junctions after 2 ms at zero bias, then returning to $V=0$ at the end of the pulse. (A) $PPF/FL/TiO_2/Au$, 100 ms pulses with the amplitudes shown. (B) Same as (A), but with expanded time scale to show initial current spike at $t=2$ ms. (C) comparison of 10 ms pulses to FL/TiO_2, Al_2O_3/TiO_2, and TiO_2 junctions. The pulse amplitude was +3 V for Al_2O_3 and FL junctions, +2 V for TiO_2.

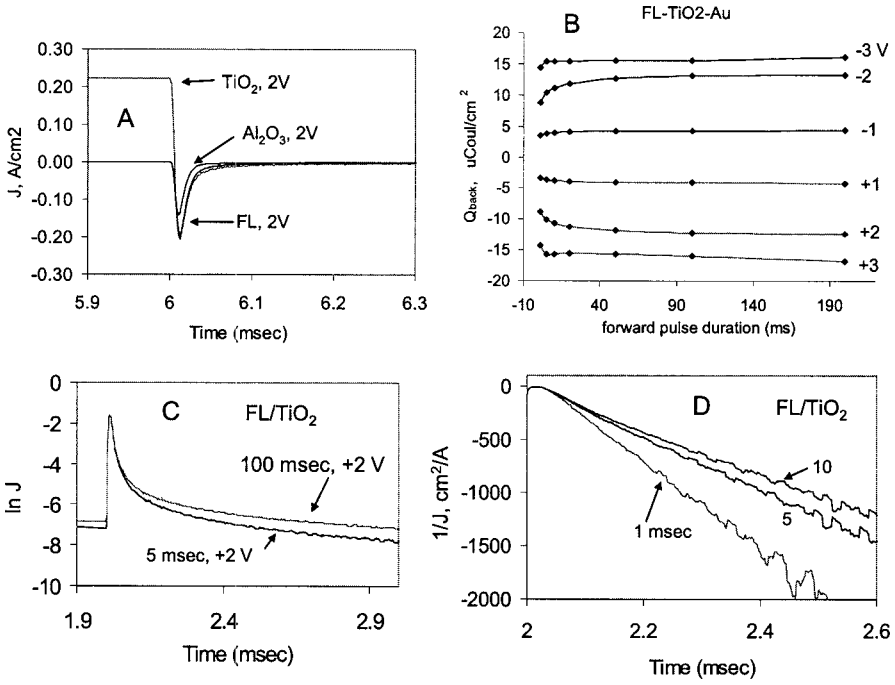

FIG. 6. Backstep pulse results for various junctions and pulse times. (A) Three TiO_2 containing junctions, forward pulse amplitude of +2 V, 5 ms, then return to $V=0$ at 6 ms. (B) Backstep pulse area in $\mu C/cm^2$ as a function of forward pulse time and voltage. (C) plot of $\ln(J)$ for backstep for 2 V forward pulses of 5 and 100 ms durations. Time axis was offset so backstep started at 2 ms to permit comparison. (D) Plots of $1/J$ vs time for backsteps of the indicated duration, with time axes offset so backstep started at 2 ms.

For the moment, we focus on the fast transient current lasting $<300\ \mu s$. This transient is more easily observed as the "backstep," when the bias is returned to zero at the end of the forward voltage pulse. Since $V=0$ at this point, there is no DC current through the junction and only the fast transient is observed. Overlays of three backstep transients following 5 ms forward pulses to +2 V are shown for the three junction types in Fig. 6(A), showing only the weak dependence on composition as long as TiO_2 was present. The magnitude of the backstep was independent of whether the slow "rise" in current was observed during the forward voltage pulse. Figure 5(B) shows the integrated area of the backstep for a FL/TiO_2 junction as a function of both voltage and forward pulse duration. Once the pulse exceeds a few milliseconds, the backstep charge is constant with pulse time, but increases with forward pulse voltage. Table I compares backstep charge for the three junction types for 100 ms pulses with several pulse amplitudes. As expected from Fig. 5(C), the backstep charge is weakly dependent on composition, varying by a factor of ~ 2 for Al_2O_3/TiO_2, FL/TiO_2, and TiO_2 junctions following +2 V pulses. In addition, the forward and backstep areas are approximately equal, although the forward area was often difficult to measure due to the rise of dc during the pulse. The magnitudes of the backstep charge vary from ~ 5 to $\sim 18\ \mu C/cm^2$ for 1–3 V pulses, with 10 $\mu C/cm^2$ corresponding to 1×10^{-10} moles/cm^2, or a density of $\sim 10^{19}\ e^-/cm^3$ in a 5 nm thick TiO_2 layer.

TABLE I. Backstep charge for 5 and 100 ms forward pulses.

			$Q_{backward}$ (C/cm^2)	
	$V_{forward}$	$Q_{forward}$ 5 ms	5 ms	100 ms
FL-TiO_2	1	2.06×10^{-6}	-3.69×10^{-6}	-4.10×10^{-6}
	2	7.17×10^{-6}	-1.02×10^{-5}	-1.22×10^{-5}
	3	[a]	-1.57×10^{-5}	-1.60×10^{-5}
TiO_2	1	5.31×10^{-6}	-6.88×10^{-6}	-8.89×10^{-6}
	2	[a]	-9.21×10^{-6}	-1.04×10^{-5}
Al_2O_3/TiO_2				
	2	2.74×10^{-6}	-5.58×10^{-6}	-6.59×10^{-6}
	3	2.78×10^{-5}	-1.06×10^{-5}	-1.83×10^{-5}
	4	6.48×10^{-5}	-2.58×10^{-5}	-3.72×10^{-5}

[a]Pulse response obscured by large dc.

It is reasonable to suppose that the "fast" current transient is simply charging current for the parallel plate capacitor comprised of PPF and Au with a single or double dielectric layer between them. However, the decay is not the expected exponential for an *RC* response, with $\ln(J)$ vs t very nonlinear [Fig. 6(C)]. The *RC* time constant for the junction area employed is $<10\ \mu s$, much faster than the observed decay. Furthermore, plots of $1/J$ vs t are linear [Fig. 8], indicating a mechanism quite different from conventional *RC* charging.

Insights into the mechanisms underlying the slow (1–100 ms) and fast (<0.1 ms) transients are provided by their temperature dependence. Figure 7(A) shows that the increase in current which occurs over a 1–100 ms time scale is strongly temperature dependent for the FL/TiO_2 junctions. Once the temperature is decreased to below $-60\ ^\circ C$, the "slow" increase is absent. However, the fast transient is nearly independent of temperature, as shown for the backstep in Fig. 7(B). The TiO_2 junctions also showed strong dependence of the slow pulse current on T, but the Al_2O_3/TiO_2 junctions had a low pulse current at all T. As shown in Fig. 7(C), the fast transient of the TiO_2 junction was weakly dependent on temperature, for both the forward and backsteps of a +1 V pulse. We attribute the fast transient to space charge capacitance associated with injection of electrons in TiO_2, as will be discussed in more detail below. After the parallel plate is charged in the first several microseconds after a positive change in bias, the space charge builds up for

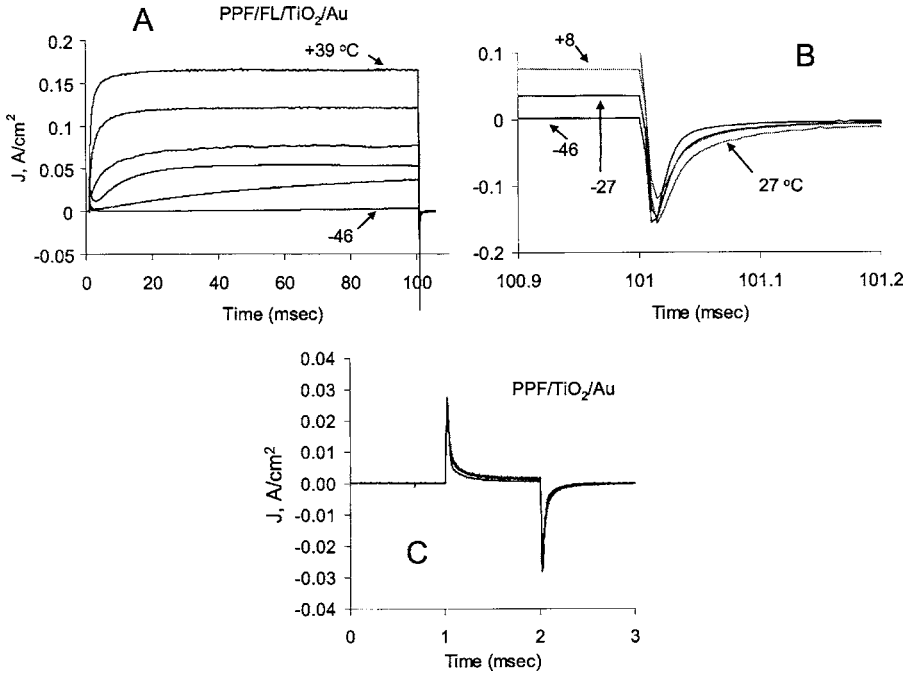

FIG. 7. Temperature dependence of pulse response of FL/TiO_2 and TiO_2 junctions. (A). $PPF/FL/TiO_2/Au$, +3 V, 100 ms pulses, in order from top to bottom: +39, +27, +8, −9, −28, and −46 °C. (B) Same data as (A), but magnified to show backstep pulses for the four temperatures indicated. (C) $PPF/TiO_2/Au$ junction, 1 ms pulses, +1 V, three temperatures superimposed: 27, −37, and −149 °C.

a few milliseconds. When the bias is returned to zero for the backstep, this space charge is dissipated over a similar approximately millisecond time scale. The result is the symmetric fast transients apparent in Figs. 5(B) and 9.

Turning our attention to the slow 1–100 ms pulse response, Fig. 10 shows the persistent changes in junction behavior following a 100 ms, +3 V pulse. The initial scan of a FL/TiO_2 junction at 1000 V/s (±2.5 V) shows low current density, consistent with Fig. 2. After a +3 V pulse lasting 100 ms, the conductance over the same voltage range increases dramatically, then fades slowly during repeated scans [Fig. 8(C)]. The conductance at $V=-2.5$ is still elevated by a factor of ~5 over its initial value of 28 min after the +3 V pulse. However, an "erase" pulse of −3 V for 100 ms immediately returns the conductance to close to its initial value [Fig. 8(B)]. The cycle of "set" (+3 V) and erase (−3 V) pulses may be repeated hundreds of times, with little change in the observed J/V curves for the set and erased states. If the duration of the +3 V set pulse is shorter, the conductance change is decreased. For a 100 ms set pulse, the conductance increases by a factor of 67 at +1.9 V, but for 11 and 1 ms pulses, this factor is reduced to 4 and 2, respectively. Therefore, the magnitude of the conductance change correlates with the slow rise in current apparent in Figs. 5(A) and 7(A), in terms of approximate time scale.

As shown in Fig. 9(A), this "memory" effect is nearly absent for the TiO_2 junction lacking fluorene. Small changes in conductance followed a +3 V or −3 V pulse, and these decayed quickly in <1 min. For the Al_2O_3/TiO_2 junction [Fig. 9(B)], the insulating Al_2O_3 reduced the currents to

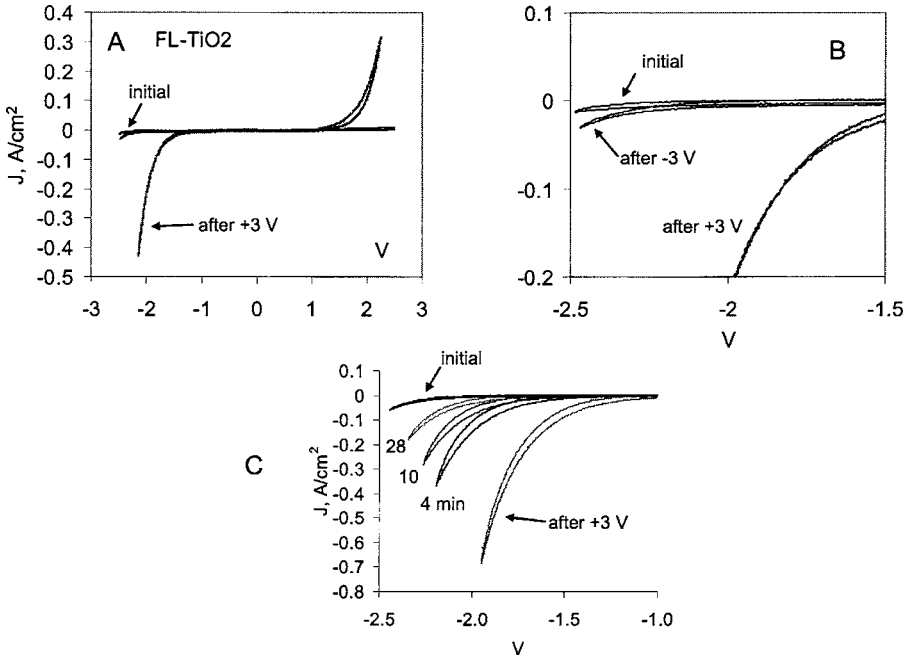

FIG. 8. Memory effect for $PPF/FL/TiO_2/Au$ junction at room temperature. 1000 V/s scans were acquired before and after 100 ms pulses to the indicated voltages. (B) is a magnified version of (A), and the −3 V pulse occurred at ~2 s after the +3 V pulse. (C) Repeated 1000 V/s scans obtained at the indicated times (in minutes) after a 100 ms, +3 V pulse. Junction was held at $V=0$ between scans.

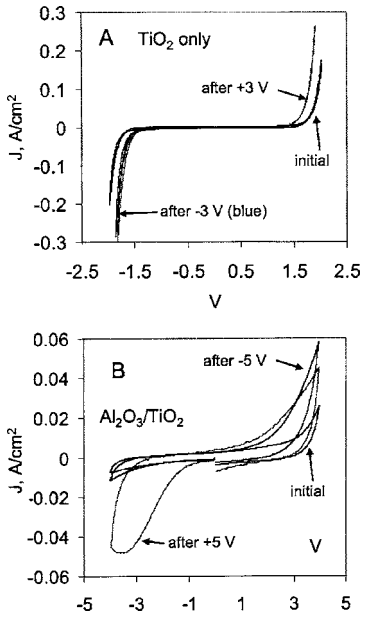

FIG. 9. Same sequence of pulses and scans as in Fig. 10 for junctions lacking fluorene. (A) PPF/TiO_2/Au, all 1000 V/s, ±3 V pulses. (B) PPF/Al_2O_3/TiO_2/Au, 1000 V/s scans initiated in negative direction, and ±5 V, 100 ms pulses.

much smaller values and persistent changes in conductance were not observed in response to set and erase pulses. However, a nonrepeatable transient current was observed on the first negative 1000 V/scan after a set pulse. The area under this peak response was approximately 8.0×10^{-5} C/cm^{-5} or 8.3×10^{-10} moles/cm^2.

DISCUSSION

Given the relatively complex structure of a PPF/FL/TiO_2/Au heterojunction, with at least three interfaces, a nanocrystalline TiO_2 layer, and a molecular monolayer to consider, there are many possible ET mechanisms which might determine the observed electronic behavior. As noted previously, Raman spectroscopy provided direct evidence for activated structural plasticity in NAB/TiO_2 and NAB/Al_2O_3 junctions under the influence of an applied bias.[14,16] In addition to structural changes, possible Schottky barriers, tunneling, traps, and redox activity could all contribute to the observed J/V response and ET mechanism(s). Several of these phenomena are illustrated in the energy level diagrams of Fig. 10 for the unbiased junctions. The levels are approximate, but are based on known values of the TiO_2 band gap (3.1 eV), the approximately equal work functions for Au and PPF (~5 eV), and the highest occupied molecular orbital–lowest unoccupied molecular orbital gap for fluorene (~5 eV). When the isolated phases shown in Fig. 10(A) are combined in a junction, some charge transfer is expected from the TiO_2 to the PPF and Au, generating Schottky barriers at each interface in a PPF/TiO_2/Au junction [Fig. 10(B)] and possibly band bending in the TiO_2. If traps are present in the TiO_2, they may depopulate and lower the contact barrier [Fig. 10(C)]. Up to this point, the junction is electrically nearly symmetric, due to the similar work functions of PPF and Au. In a FL/TiO_2 junction, the tunneling barrier generated by the fluorene layer makes the junction asymmetric, and the extent of charge transfer at the two interfaces is likely different. The result is a built-in field across the fluorene layer, as shown in Fig. 10(D).

While a comprehensive description of all ET mechanisms operative in the current junctions would require significantly more data than currently in hand, the results do permit conclusions about three regimes of the J/V response, which will be considered in turn. First, the low voltage region between −1 and +1 V exhibits low conductance at any temperature and scan rate studied. Second, a fast response over a few millisecond time scale occurs for voltage magnitudes exceeding ~1.5 V, and is weakly temperature dependent. Third, a slower and persistent change in conductance follows relatively long pulses (>1 ms) and is strongly temperature dependent. Throughout the discussion of these three regions, it is important to consider the effect of adding the

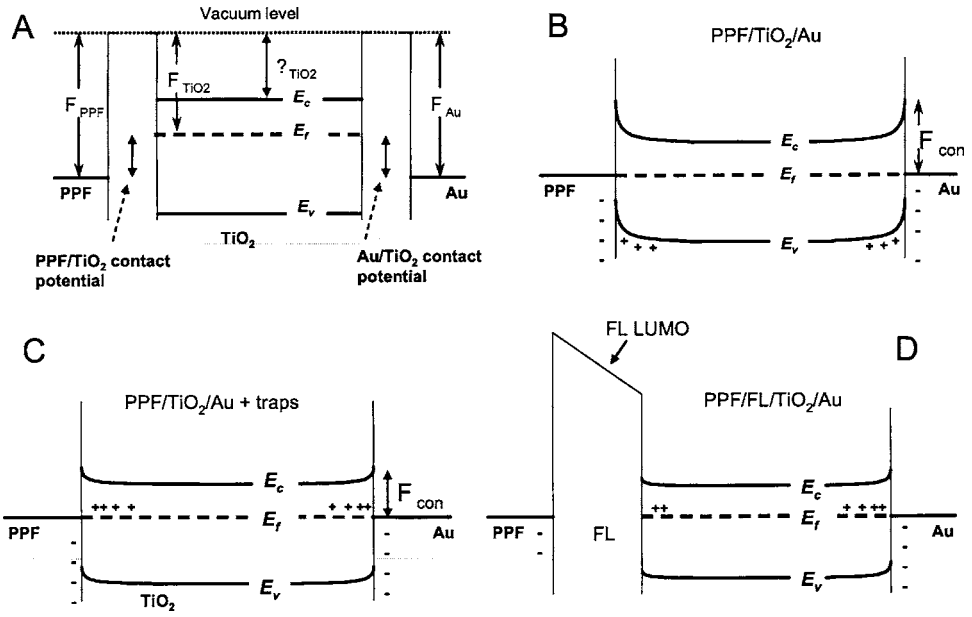

FIG. 10. Approximate energy level diagrams at zero bias for (A) isolated materials, (B) junction without traps at thermal equilibrium, (C) PPF/TiO_2/Au junction with traps in TiO_2, and (D) PPF/FL/TiO_2/Au junction. Vertical scale is electron energy referenced to the vacuum level, with higher energy upward. E_c and E_v are the TiO_2 conduction and valence band energies, Φ_{Au} and Φ_{PPF} are the Au and PPF work functions, X_{TiO_2} is the TiO_2 electron affinity, Φ_{con} is the TiO_2/Au contact barrier, and FL LUMO is the lowest unoccupied molecular orbital of fluorene. The horizontal dashed line denotes the Fermi energy E_F.

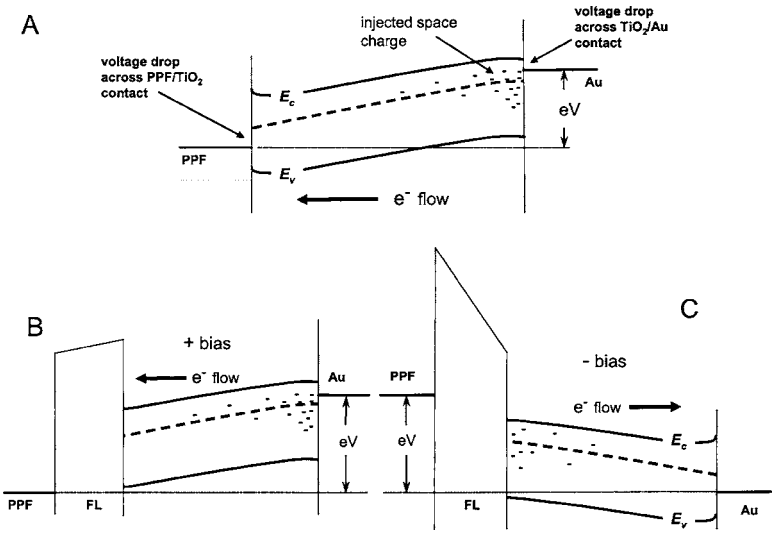

FIG. 11. Energy level diagrams under applied bias. (A) PPF/TiO_2/Au junction with positive bias (PPF positive relative to Au), (B) PPF/FL/TiO_2/Au junction under positive bias, and (C) PPF/FL/TiO_2/Au junction under negative bias. The dashed lines denote the quasi-Fermi-level for electrons for the biased junctions.

fluorene layer to the PPF/TiO_2/Au junction, which introduces structural asymmetry into the junction structure.

The junction resistance at low voltage is high in the range of 10^4–10^5 $\Omega\,cm^2$ or 2–20 MΩ for the 0.005 cm^2 junction area. At 1000 V/s, a capacitive current component is observable, yielding a junction capacitance which decreases with both faster scan rate and lower temperature. The capacitance at 1000 V/s and $V=0$ is approximately 0.9 $\mu F/cm^2$ for a FL/TiO_2 junction, yielding an average dielectric constant of 7.2 based on a parallel plate capacitor model with a thickness of 6.8 nm. A coherent tunneling mechanism based on the Simmons formula[24] yields a predicted low voltage resistance of $>10^{12}$ $\Omega\,cm^2$ for a 6.8 nm thick junction and unreasonably low barrier height of 0.5 eV. Furthermore, coherent tunneling would be neither scan rate nor temperature dependent. Therefore, the low voltage J/V behavior for the $V=\pm 1$ V range cannot be explained by conventional tunneling, and other phenomena must be involved. Furthermore, a proposed mechanism must also account for the variation of both low voltage resistance and capacitance with scan rate and temperature.

The anomalous behavior of the capacitance with scan rate and temperature and the transient response to voltage pulses [Figs. 6(C) and 6(D)] are inconsistent with a conventional parallel plate capacitor. It is apparent from Table I that the "backstep charge" stored in the junction during the voltage pulse is not greatly affected by the presence of the fluorene or Al_2O_3 layers, and is independent of whether the junction exhibits dc conduction. These observations are consistent with a conductance mechanism operative in semiconductors and insulators, i.e., space charge limited conduction (SCLC).[25–27] As the bias increases, electrons are injected into the TiO_2 to form a space charge, with electrons located both in the TiO_2 interior and at the conductor/TiO_2 interfaces. In the simplest case of a perfect crystal, this space charge provides carriers in the conduction band, and the current density follows Child's law,

$$J = \frac{9\mu\epsilon V^2}{8d^3}, \tag{1}$$

where μ is the mobility ($cm^2\,V^{-1}\,s^{-1}$), $\in$ is the permittivity ($F\,cm^{-2}$), and d is the junction thickness (cm).

Considering the case of PPF/TiO_2/Au initially, the flat J/V curve below $|V|=1.5$ V implies that few electrons are injected into the TiO_2, presumably because the potential is insufficient to overcome the contact barriers at the PPF/TiO_2 and Au/TiO_2 interfaces. Figure 11(A) shows a modification of Fig. 10(C) for the case of an applied bias. As the bias magnitude is increased beyond 1.5 V, the contact barrier becomes small enough that electron injection builds up a space charge in the form of conduction band electrons, hence more mobile charge carriers are available, and the current increases. However, the increase in current with bias is much faster than predicted by the V^2 dependence of Eq. (1). For example, the slope of ln(J) vs ln(V) for a TiO_2 junction [Fig. 4(D)] is 11.4 at 25 °C and 10.5 at −135 °C, for the voltage range where J exceeds 7 mA/cm^2. For a FL/TiO_2 junction, the slope is ~26 at 25 °C and ~12 at −139 °C. Since Eq. (1) predicts a slope of 2 for ln(J) vs ln(V), SCLC is not a sufficient explanation for the observed J/V behavior. In addition, SCLC alone should not exhibit the hysteresis which is clearly evident in the J/V curves at room temperature.

A modification of the basic SCLC mechanism includes "traps," i.e., localized energy states which capture an otherwise mobile electron and prevent it from participating in conduction.[26,27] Nanocrystalline TiO_2 is known to contain numerous traps, presumably at grain boundaries and other defects.[11,28,29] Lampert[27] provides a detailed description of the effect of traps on SCLC and discusses a "trap-filled limit" which is the voltage where enough electrons have been captured to fill all of the energetically accessible traps. At this voltage, the current increases rapidly from Ohmic behavior (ln J vs ln V slope=1) to Child's law behavior, and can result in the large values of d(ln J)/d(ln V) apparent in Fig. 6(B). Since traps generally involve some nuclear reorganization in response to capture of an electron, they have an activation energy as well as a depth, and exhibit kinetics and temperature dependence. Although several reports estimate the trap depth in nanocrystalline TiO_2 to be 0.5–0.8 eV below the conduction band edge,[29,30] there is likely to be a fairly wide distribution of trap energies. When traps with finite kinetics are included in the model, we can account for the J/V hysteresis as well as the sharp increase in current at high bias. When the scan rate is fast (1000 V/s), the traps do not have

time to fill, and few injected electrons are trapped. At slow scan rates (e.g., 10 V/s), the traps equilibrate with the local Fermi level, and the sharp current increase is observed as most of the energetically accessible traps become filled. At intermediate scan rates (~100 V/s), the traps are filling on a time scale comparable to the scan rate, and hysteresis is observed as detrapping time causes the current to lag the voltage after the scan is reversed.

Many traps in TiO_2 should be accessible in the absence of dc conduction, in junctions with fluorene or Al_2O_3 layers, or TiO_2 alone. As the Fermi level in the TiO_2 increases near the negatively biased electrode, traps will start to fill regardless of DC current flow. The behavior of Al_2O_3/TiO_2 junctions is informative in this case because the only current observed is that associated with parallel plate and space charge capacitance. We attribute the peak in the J/V curve of an Al_2O_3/TiO_2 junction in Fig. 3(B) at $V=-3$ V to the "detrapping" of electrons injected during the positive scan, when Au was negative. Furthermore, we assert that the backstep charge tabulated in Table I and the unusual current decay apparent in Figs. 6(C) and 6(D) arise mostly from trapped charge, not only because the rate of charge decay is too slow to be consistent with the RC time constant of the structure but also because the time dependence of the current response cannot be explained without the introduction of an energetic barrier to impede the normal resistive decay of the space charge.

A model based on SCLC with traps accounts for most of the experimental observations, including the sharp increase in current at the trap filled limit, the hysteresis, and the trends observed in the backstep charge with changes in composition, time, and pulse voltage. However, the slow (1–100 ms) rise in current [Fig. 5(A)] and memory effect lasting several minutes (Fig. 8) are not consistent with a mechanism based solely on SCLC and traps. The voltammetry and pulse experiments indicate that charge injection and trapping occur in a few milliseconds, and the space charge is dissipated in much less than 10 ms after the bias is returned to zero (Fig. 6). The slow rise in current is strongly temperature dependent, while the submillisecond transients are not. The dc conductance changes and memory effect are strongly dependent on junction composition [Fig. 5(C)], while the transient current and charge vary by only a factor of ~2 for FL/TiO_2, Al_2O_3/TiO_2, and TiO_2 only junctions. The pronounced differences in time scale and dependence on junction structure require an additional phenomenon to be considered, other than SCLC with traps.

Consider again the pulse responses of Figs. 5(A) and 5(C), and the memory effect shown in Figs. 8 and 9. For the Al_2O_3/TiO_2 junction, only the transient current is observed, since DC current is blocked by the Al_2O_3 layer. For the TiO_2 junction, electron injection begins from either Au or PPF when the voltage is high enough to overcome the contact barriers shown in Fig. 11(A), and the traps begin to fill. A steady state is reached in which electrons enter and exit the TiO_2 at the same rate, and the quasi-Fermi-level of the TiO_2 does not undergo a large net change. When the bias is returned to zero, the traps empty, and there is no persistent memory effect. The junction behaves as if it were electronically symmetric, implying that the barriers present at the PPF/TiO_2 and TiO_2/Au interfaces are similar, as expected from the approximately equal work functions of PPF and Au. Introduction of the fluorene layer to make a $PPF/FL/TiO_2/Au$ junction makes the junction structurally asymmetric, but unlike Al_2O_3, the FL layer does not block DC conduction. During positive bias, the Au/TiO_2 interface is negative and electrons are injected into the TiO_2. The space charge builds up, with trapping until tunneling across the fluorene layers equals the rate of electron injection [Fig. 11(B)]. The requirement for a relatively high field to tunnel through the fluorene layer has the effect of increasing the TiO_2 Fermi level. We propose that this high Fermi level causes a relatively slow reduction reaction in the TiO_2 to produce a Ti^{III} or Ti^{II} oxide. Alternatively, the rate of oxidation at the positive electrode in a $PPF/TiO_2/Au$ junction may equal the rate of reduction at the negative electrode, and this balance may be disturbed by the addition of the FL layer. There are several possibilities for a reduction reaction such as

$$2TiO_2 + H_2O + 2e^- \rightarrow Ti_2O_3 + 2OH^-, \tag{2}$$

$$2TiO_2 + 2e^- \rightarrow Ti_2O_3 + O^{-2}. \tag{3}$$

An alternative representation more common for solid state reactions uses Kröger-Vink notation,[31,32] as in reactions

$$Ti_{Ti} + 2O_O + V_I \rightarrow O_2 + Ti_I^{\cdots\cdot} + 4e', \tag{4}$$

$$V_I + TiO_2 \rightarrow Ti_I^{\cdot\cdot} + O_2 + 2e', \tag{5}$$

The Kröger-Vink notation specifically identifies conduction band electrons (e'), as well as denoting vacancies (V) and interstitials (subscript I). Reaction (5) was proposed by Knauth and Tuller[32] to explain the increased conductivity of TiO_2 under low partial pressure of O_2, While reactions (2)–(5) differ with respect to the products of reduction, they all yield mobile electrons in the conduction band. The reactions obviously involve structural rearrangements, and will have associated activation barriers and temperature dependence. After the bias is returned to $V=0$, any space charge will dissipate in a few milliseconds, but the Ti_2O_3 will persist, although the reaction will eventually reverse at a rate controlled by its activation energy.

The major consequence of Ti_2O_3 generation is its much higher conductivity compared to TiO_2 by approximately ten orders of magnitude.[13,14,16] The conduction band electrons associated with Ti_2O_3 are mobile, and the TiO_2 is effectively "doped" to become a n-type semiconductor. As is apparent from Fig. 2(A), the fluorene layer can support high current densities in PPF/FL/Cu junctions, so an increase in conduction of the TiO_2 layer will lead to an overall increase in junction conductance. In the case of the $PPF/TiO_2/Au$ junction, the reduction process is less pronounced, presumably because the TiO_2 layer cannot become sufficiently negative. Although ET through the TiO_2 is more efficient than through FL/TiO_2, the lack of the FL tunneling barrier diminishes the increase in the local Fermi level in the TiO_2, thus decreasing the driving force for TiO_2 reduction. With the FL absent, the memory effect is weak, implying that TiO_2 reduction is re-

quired for persistent conductance changes. Once the high conductance state is produced by TiO_2 reduction, it may be erased by a negative voltage pulse as shown in Figs. 10(A) and 10(C) and schematically in Fig. 11(C). During the erase pulse, the Au is positive, the quasi-Fermi-level in the TiO_2 decreases, and reactions (2) and (3) should reverse, thus re-oxidizing Ti_2O_3. In effect, the reduction of TiO_2 by the accumulated space charge is a form of "dynamic doping," in which the conductance of the oxide is dramatically increased by a positive bias, through generation of Ti_2O_3. The fluorene layer permits the oxide to partially "float" relative to the PPF, so that the quasi-Fermi-level can track the Au potential.

It is well known that various types of "breakdown" can occur in insulators under an imposed electric field, and such effects have been reported for TiO_2 (Ref. 33) and metal/molecule junctions containing Ti.[34] Loosely speaking, the redox mechanism described here is a type of breakdown, in that the initially insulating oxide is made conductive by injection of electrons, and the oxide structure is modified. However, the redox modulation of conductance is reversible for at least hundreds of cycles, and may be driven to high and low states depending on bias polarity. Therefore, it differs fundamentally from conventional dielectric breakdown mediated by pinhole formation or local thermal transients. It is not yet known if the conductance paths formed by the redox process are localized, but the proposed mechanism is consistent with homogeneous generation of Ti^{III} sites, with accompanying generation of conduction band electrons.

As discussed in previous reports,[6,13,14,16] the role of ion motion and impurities in the TiO_2 and/or molecular layer is not clear. It is possible that a reduction reaction such as Eqs. (2) and (3) could be "balanced" by an image charge in the PPF, effectively stabilizing the space charge with a high electric field. Alternatively, the injected electrons may originate in the molecular layer, as was demonstrated spectroscopically for PPF/NAB/TiO_2/Au junctions.[16] Fluorene has a high redox potential for oxidation to a radical cation ($>+2$ V), so its participation in redox reactions is less likely than NAB. Additional spectroscopic experiments are presently underway to determine the conditions required for TiO_2 reduction by using UV-Vis absorption to monitor the TiO_2 redox state. Whether or not mobile ions are involved, it is reasonable to propose that reactions such as Eq. (2) or (3) above may be driven by a high electron density in the TiO_2 layer, in a manner similar to a conventional electrochemical reduction. The current work supports and elaborates previous conclusions that the principal effect of an applied bias on conductance is modulation of the TiO_2 electronic properties.[13–16] The effects of charge balance, ion motion, and image charges on junction electronic behavior are topics of current investigation.

ACKNOWLEDGMENTS

This work was supported by the National Science Foundation through project 0211693 from the Analytical and Surface Chemistry Division, and by ZettaCore, Inc.

[1] J. Jortner and M. Ratner, *Molecular Electronics* (Blackwell Science, Oxford, UK, 1997).
[2] J. R. Heath and M. A. Ratner, Phys. Today **56** (5), 43 (2003); C. R. Kagan and M. A. Ratner, MRS Bull., 376 (June, 2004).
[3] L. A. Bumm, J. J. Arnold, M. T. Cygan, T. D. Dunbar, T. P. Burgin, L. Jones, D. L. Allara, J. M. Tour, and P. S. Weiss, Science **271**, 1705 (1996); Z. J. Donhauser, B. A. Mantooth, K. F. Kelly *et al.*, *ibid.* **292**, 2303 (2001); A. M. Rawlett, T. J. Hopson, L. A. Nagahara, R. K. Tsui, G. K. Ramachandran, and S. M. Lindsay, Appl. Phys. Lett. **81**, 3043 (2002); G. K. Ramachandran, T. J. Hopson, A. M. Rawlett, L. A. Nagahara, A. Primak, and S. M. Lindsay, Science **300**, 1413 (2003); F. Chen, J. He, C. Nuckolls, T. Roberts, J. Klare, and S. M. Lindsay, Nano Lett. **5**, 503 (2005); F.-R. F. Fan, R. Y. Lai, J. Cornil *et al.*, J. Am. Chem. Soc. **126**, 2568 (2004); X. Xiao, B. Xu, and N. J. Tao, Nano Lett. **4**, 267 (2004); Y. Xue, S. Datta, S. Hong, R. Reifenberger, J. I. Henderson, and C. P. Kubiak, Phys. Rev. B **59**, R7852 (1999); S. Datta, W. Tian, S. Hong, R. Reifenberger, J. I. Henderson, and C. P. Kubiak, Phys. Rev. Lett. **79**, 2530 (1997).
[4] S. M. Lindsay, Electrochem. Soc. Interface **13**, 26 (2004).
[5] D. L. Feldheim, K. C. Grabar, M. J. Natan, and T. E. Mallouk, J. Am. Chem. Soc. **118**, 7640 (1996); D. Vuillame, B. Chen, and R. M. Metzger, Langmuir **15**, 4011 (1999); R. M. Metzger, T. Xu, and I. R. Peterson, J. Phys. Chem. B **105**, 7280 (2001); L. T. Cai, H. Skulason, J. G. Kushmerick, S. K. Pollack, J. Naciri, R. Shashidhar, D. L. Allara, T. E. Mallouk, and T. S. Mayer, *ibid.* **108**, 2827 (2004).
[6] R. L. McCreery, U. Viswanathan, R. P. Kalakodimi, and A. M. Nowak, Faraday Discuss. **131**, 33 (2006).
[7] M. Galperin, A. Nitzan, M. A. Ratner, and D. R. Stewart, J. Phys. Chem. B **109**, 8519 (2005); M. Galperin, M. Ratner, and A. Nitzan, Nano Lett. **4**, 1605 (2004); M. L. Chabinyc, X. Chen, R. Holmlin, H. Jacobs, H. Skulason, C. D. Frisbie, V. Mujica, M. Ratner, M. A. Rampi, and G. M. Whitesides, J. Am. Chem. Soc. **124**, 11730 (2002); A. Nitzan, J. Jortner, J. Wilkie, A. L. Burin, and M. A. Ratner, J. Phys. Chem. B **104**, 5661 (2000); D. Segal, A. Nitzan, M. Ratner, and W. D. Davis, *ibid.* **104**, 2790 (2000).
[8] R. McCreery, Chem. Mater. **16**, 4477 (2004).
[9] R. M. Metzger, Chem. Rev. (Washington, D.C.) **103**, 3803 (2003); R. M. Metzger, Electrochem. Soc. Interface **13**, 43 (2004).
[10] K.-Y. Tse, B. M. Nichols, W. Yang, J. E. Butler, J. N. Russell, Jr., and R. J. Hamers, J. Phys. Chem. B **109**, 8523 (2005); P. T. Hurley, A. E. Ribbe, and J. M. Buriak, J. Am. Chem. Soc. **125**, 11334 (2003); C. A. Hacker and R. J. Hamers, J. Phys. Chem. B **107**, 7689 (2003); M. P. Stewart and J. M. Buriak, Comments Inorg. Chem. **23**, 179 (2002); L. Fang, J. Liu, S. Coulter, X. Cao, M. P. Schwartz, C. Hacker, and R. J. Hamers, Surf. Sci. **514**, 362 (2002); M. P. Stewart, F. Maya, D. V. Kosynkin, S. M. Dirk, J. J. Stapleton, C. L. McGuiness, D. L. Allara, and J. M. Tour, J. Am. Chem. Soc. **126**, 370 (2004).
[11] D. Kuciauskas, M. S. Freund, H. B. Gray, J. R. Winkler, and N. S. Lewis, J. Phys. Chem. B **105**, 392 (2001).
[12] M. K. I. Senevirathna, P. K. D. D. P. Pitigala, V. P. S. Perera, and K. Tennakone, Langmuir **21**, 2997 (2005); N. M. Dimitrijevic, Z. V. Saponjic, D. M. Bartels, M. C. Thurnauer, D. M. Tiede, and T. Rajh, J. Phys. Chem. B **107**, 7368 (2003); S. Nakade, M. Matsuda, S. Kambe, Y. Saito, T. Kitamura, T. Sakata, Y. Wada, H. Mori, and S. Yanagida, *ibid.* **106**, 10004 (2002); G. P. Mitchell, C. A. Mirkin, and R. L. Letsinger, J. Am. Chem. Soc. **121**, 8122 (1999); L. G. Quagliano, *ibid.* **126**, 7393 (2004); L. Jingbo and L. W. Wang, Chem. Mater. **16**, 4012 (2004).
[13] R. McCreery, J. Wu, and R. J. Kalakodimi, Phys. Chem. Chem. Phys. **8**, 2572 (2006).
[14] R. P. Kalakodimi, A. Nowak, and R. L. McCreery, Chem. Mater. **17**, 4939 (2005).
[15] W. R. McGovern, F. Anariba, and R. McCreery, J. Electrochem. Soc. **152**, E176 (2005).
[16] A. Nowak and R. McCreery, J. Am. Chem. Soc. **126**, 16621 (2004).
[17] R. McCreery, in *Molecular Electronics*, special issue of Electrochem. Soc. Interface **13**, 46 (2004).
[18] R. L. McCreery, J. Dieringer, A. O. Solak, B. Snyder, A. Nowak, W. R. McGovern, and S. DuVall, J. Am. Chem. Soc. **125**, 10748 (2003).
[19] W.-J. Yoon, S.-Y. Chung, P. Berger, and S. M. Asar, Appl. Phys. Lett. **87**, 203506 (2005).
[20] F. Anariba, J. Steach, and R. McCreery, J. Phys. Chem. B **109**, 11163 (2005).
[21] S. Ranganathan and R. L. McCreery, Anal. Chem. **73**, 893 (2001); S. Ranganathan, R. L. McCreery, S. M. Majji, and M. Madou, J. Electrochem. Soc. **147**, 277 (2000).
[22] F. Anariba, S. H. DuVall, and R. L. McCreery, Anal. Chem. **75**, 3837

(2003); F. Anariba, U. Viswanathan, D. F. Bocian, and R. L. McCreery, *ibid.* **78**, 3104 (2006).
[23] R. McCreery, J. Dieringer, A. O. Solak, B. Snyder, A. M. Nowak, W. R. McGovern, and S. DuVall, J. Am. Chem. Soc. **126**, 6200 (2004).
[24] J. G. Simmons, *DC Conduction in Thin Films* (Mills and Boon, London, 1971); D. R. Lamb, *Electrical Conduction Mechanisms in Thin Insulating Films* (Methuen and Co., London, 1968).
[25] S. M. Sze, *The Physics of Semiconductor Devices*, 2nd ed. (Wiley, New York, 1981); P. Mark, J. Appl. Phys. **33**, 205 (1962); M. A. Lampert and P. Mark, *Current Injection in Solids* (Academic, London, 1970).
[26] J. Sworakowski, J. Appl. Phys. **41**, 292 (1970); J. Sworakowski and K. Pigon, J. Phys. Chem. Solids **30**, 491 (1969).
[27] M. Lampert, Phys. Rev. B **103**, 1648 (1956).
[28] T. Bak, J. Nowotny, M. Rekas, and C. C. Sorrell, J. Phys. Chem. Solids **63**, 1069 (2003); J. Nelson, A. M. Eppler, and I. M. Ballard, J. Photochem. Photobiol., A **148**, 25 (2002); V. Mikhelashvili and G. Eisenstein, J. Appl. Phys. **89**, 3256 (2001).
[29] S. Leytner and J. T. Hupp, Chem. Phys. Lett. **330**, 231 (2000).
[30] M. Bailes, P. J. Cameron, K. Lobato, and L. M. Peter, J. Phys. Chem. B **109**, 15429 (2005).
[31] D. M. Smith, *The Defect Chemistry of Metal Oxides* (Oxford University Press, New York, 2000).
[32] P. Knauth and H. L. Tuller, J. Appl. Phys. **85**, 897 (1999).
[33] B. J. Choi, D. S. Jeong, S. K. Kim *et al.*, J. Appl. Phys. **98**, 033715 (2005).
[34] C. N. Lau, D. R. Stewart, M. Bockrath, and R. S. Williams, Appl. Phys. A: Mater. Sci. Process. **A80**, 1373 (2005).